

A Shell Source Model for Red Giant Stars

G. GAMOW AND G. KELLER

The George Washington University, Washington, D. C.

1. INTRODUCTION

IT is generally accepted at present that the stars of the main sequence, or rather the stars in the main sequence stage of their evolution, owe their energy supply to the so-called C-N cycle¹ (transformation of hydrogen into helium through the catalytic action of carbon and nitrogen) taking place in the center of the star. This leads to Cowling's semiconvective point source model,² consisting of a central convective zone and an outer envelope in a state of radiative equilibrium. The introduction of the convective zone in the point source model is necessitated by the fact that the radiative equilibrium of the stellar material becomes unstable at a certain distance from the center and must break up into a series of convective currents. The continuous circulation of the material within the convective core of the star insures its uniform chemical constitution, the changes taking place in the center as a result of nuclear transformations being distributed rapidly through the entire core. If we assume, as it is usually done, that the stellar material originally contains about 35 percent hydrogen (the rest being a mixture of heavier elements), and that this hydrogen is later completely transformed into helium, the molecular weight of the convective core will increase gradually from a value of about 1 to a value of about 2. The effect of these evolutionary changes on the observable characteristics of the star have been studied in some detail by Miss Harrison.³ It has been shown by this author that the increase of molecular weight μ from 1 to 2 leads to a shrinking of the convective core, and a steady increase of the stellar radius and luminosity. The resulting evolutionary curve in the frame of a $(\log L/L_{\odot}$ vs. $\log R/R_{\odot})$ -diagram is shown in Fig. 1, where L/L_{\odot} and R/R_{\odot} are the

luminosity and radius of the star, respectively, expressed in solar units.⁴ As the hydrogen content of the convective core decreases, the temperature of this region must rise steadily in order to insure the proper rate of energy production, which, as it is easy to see, will result in the appearance of new sources just outside the convective region where the hydrogen content is still high and the gradual fading of the central source of energy. When the hydrogen content of the convective core finally drops to zero, the production of energy within the core ceases. The currents then stop because of the lack of a driving force, and the temperature becomes constant throughout the core. Thus the structure of the star is gradually transformed into that of the so-called *shell source model*, with an isothermal core of dehydrogenized material, a thin energy producing layer, and a radiative envelope with

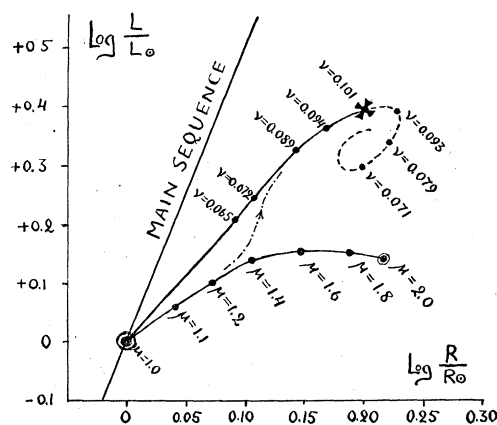


FIG. 1. The evolutionary tracks of a Cowling model star with increasing molecular weight μ of the convective core (after Miss Harrison), and that of a shell source model star with an increasing fraction of the total mass in the isothermal core (after Schönberg and Chandrasekhar). L/L_{\odot} and R/R_{\odot} are the luminosity and radius of the star respectively, expressed in solar units.

¹ C. v. Weizsäcker, *Physik. Zeits.* **39**, 633 (1938); H. Bethe, *Phys. Rev.* **55**, 434 (1939).

² Cowling, *M. N. R. A. S.* **96**, 42 (1936).

³ Marjorie H. Harrison, *Astrophys. J.* **100**, 343 (1944).

⁴ The curve in Fig. 1 is calculated under the assumption of a constant central temperature of the convective core; the steady increase in this temperature will result in somewhat smaller changes in the stellar radius.

the original high hydrogen content.⁵ The further evolution of the star must now proceed in the direction of a continuous growth of the energy producing shell towards the surface of the star. The upper line in Fig. 1 gives the evolutionary track of such a star as that calculated by Schönberg and Chandrasekhar under the assumption of $\mu=2$ for the isothermal core and $\mu=1$ for the envelope. The transition from the semiconvective point source model to the shell source model is indicated schematically by the dot dashed line.

In their study of the evolution of a shell source model of a star the above authors came to a peculiar result, namely, that no solutions exist which correspond to an equilibrium condition of the star when the amount of matter in the core exceeds 10 percent of the total mass of the star.⁶ This is illustrated in Fig. 1 by the broken line continuation of the evolutionary track, the points of which correspond to decreasing values of the mass of the dehydrogenized isothermal core. Since physically the mass of the core must increase continually, the above result lead these authors to the conclusion that beyond the 10 percent point on the evolutionary curve (marked with a cross in Fig. 1) the star must evolve through a series of non-equilibrium configurations which they try to connect with the phenomena of stellar explosions.

It has recently indicated by one of us⁷ that the above result concerning the upper limit for the isothermal core does not necessarily represent an intrinsic property of the shell source stellar model, but may be due in part to the arbitrary assumption made in the calculations that the gas forming the isothermal core is always ideal. By taking into account the possibility that degeneracy may occur in the center of a core with a fixed temperature and steadily increasing

density, the picture changes considerably. Because of the degenerate condition, stellar models obtained in this way are not subject to the homology transformations in respect to the mass. Consequently the fitting of semidegenerate cores to radiative envelopes must be carried out individually for any particular star mass. In fact, as we shall see later, one obtains entirely different evolutionary tracks for large and small stellar masses.

In the present article we will consider the fitting of partially degenerate cores of fixed temperature $T^*=2\times 10^7$ °K (corresponding to the C-N cycle in the energy producing shell) and molecular weight $\mu_{\text{core}}=2$ to radiative envelopes of molecular weight $\mu_{\text{env}}=1$ and opacity coefficient $k_0=7.1\times 10^{24}$ ($\log k_0=24.85$). The value of the molecular weight chosen for the envelope corresponds to a hydrogen content of 35 percent. The fitting method consists in "cutting out" from isothermal solutions with varying central densities cores of the desired mass M^* , and fitting these cores to envelopes obtained from various radiative equilibrium solutions for the given star mass M . In order to make the envelope fit, a mass is cut out of its center equal to that of the isothermal core. The fitting conditions are that the gas pressure and temperature must be continuous at the interface between the isothermal and radiative parts.

2. SOLUTIONS FOR ISOTHERMAL CORES

We will first discuss the method of building isothermal cores both for the case of an ideal gas and a partially degenerate gas.

A. The Case of an Ideal Gas

The equilibrium equation for an isothermal sphere of an ideal gas can be written in the form⁸

$$dp/dr = -G\rho M(r)/r^2, \quad (1)$$

where

$$M(r) = \int_0^r 4\pi\rho r^2 dr; \quad (2)$$

and

$$p = (R/\mu)\rho T^*, \quad (3)$$

where p = gas pressure, r = the radius, ρ = the density, $M(r)$ = the mass within the radius r ,

⁵ G. Gamow, *Astrophys. J.* **87**, 206 (1938); Chas. Critchfield and G. Gamow, *Astrophys. J.* **89**, 244 (1939); R. Henrich and S. Chandrasekhar, *Astrophys. J.* **94**, 525 (1941); M. Schönberg and S. Chandrasekhar, *Astrophys. J.* **96**, 161 (1942).

⁶ A similar result had been obtained previously by Henrich and Chandrasekhar (reference 5) for models in which the molecular weight of the core remains the same as that of the envelope. In this case, however, the solutions were non-existent only when the core exceeded 35 percent of the star mass.

⁷ G. Gamow, *Phys. Rev.* **67**, 120 (1945).

⁸ Radiation pressure neglected.

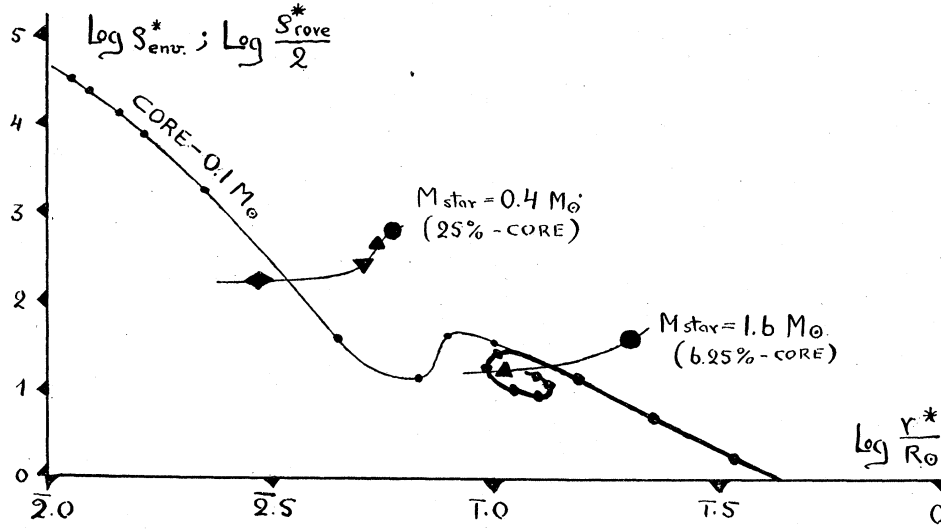


FIG. 2. Fitting curves for a core of mass $M^* = 0.1 M_\odot$ and for the corresponding envelopes pertaining to the stars of total mass equal to 0.4 and $1.6 M_\odot$. We notice that in the first case (6.25 percent core) an intersection is obtained with the ideal gas part of the curve (heavy line), whereas in the second (25 percent core) the intersection corresponds to a partially degenerated core. The black circles, triangles, inverted triangles, and diamonds correspond to points of the envelope fitting curves obtained respectively from Cowling's convective solution, from two solutions given by Strömgen, and from the solution given in Table I.

G = gravitational constant, μ = the molecular weight at the radius r , T^* = the temperature of the isothermal core and energy producing shell, and R = the gas constant. The boundary conditions are

$$\rho = \rho_c; \quad d\rho/dr = 0 \quad (4)$$

at the center. Since T^* is constant the above equations can be rewritten in the form

$$\frac{1}{r^2} \frac{d}{dr} \left(r^2 \frac{d \log \rho}{dr} \right) = - \frac{4\pi G \mu \rho}{RT^*} \quad (5)$$

Introducing new variables ξ and v connected with the old ones by the relations

$$r = \xi/\alpha, \quad (6)$$

$$\rho = \rho_c e^{-v}, \quad (7)$$

$$\alpha^2 = 4\pi G \mu \rho_c / RT^*, \quad (8)$$

where

the Eq. (5) may be transformed to

$$\frac{1}{\xi} \frac{d}{d\xi} \left(\xi^2 \frac{dv}{d\xi} \right) = e^{-v} \quad (9)$$

with the boundary conditions

$$v = dv/d\xi = 0 \quad \text{at} \quad \xi = 0. \quad (10)$$

The mass within the radius r is expressed in new

variables by the formula

$$M(r) = \frac{RT^*}{\mu \alpha G} \frac{dv}{d\xi} \xi^2. \quad (11)$$

Equation (9) describes the polytrope of index $K=1$ and $n=\infty$, and its solutions have been tabulated by Emden.⁹ Using (6) and (11) we obtain

$$M(r) = \frac{RT^*}{\mu G} r \cdot \xi \frac{dv}{d\xi}. \quad (12)$$

On the other hand from (6), (7), and (8) we have

$$\rho = \rho_c e^{-v} = \frac{RT^* \alpha^2}{4\pi G \mu} e^{-v} = \frac{RT^*}{4\pi G \mu} \frac{1}{r^2} \xi^2 e^{-v}. \quad (13)$$

Taking $M(r)$ equal to the desired mass M^* of the core, adjusting r and ρ to the desired values r^* and ρ^* for the radius and the density on the surface of the core, and expressing all in terms of the mass M_\odot and radius R_\odot of the sun, we can rewrite the above two equations in the form

$$\frac{r^*}{R_\odot} = \left(\frac{M^*}{M_\odot} \right) \left(\frac{\mu G}{RT^*} \right) \frac{M_\odot}{R_\odot} \left[\xi \frac{dv}{d\xi} \right]^{-1} \quad (14)$$

⁹ A table of these solutions can be found for example in Milne, *Handbuch d. Astrophys.* They were originally given in R. Emden, *Gaskugeln* (B. G. Teubner, Leipzig, 1907), where a somewhat different notation is employed from that used here.

and

$$\rho^* = \frac{1}{4\pi M_\odot^2} \left(\frac{RT^*}{\mu G} \right)^3 \left(\frac{M^*}{M_\odot} \right)^{-2} \left[\frac{dv}{d\xi} \right]^2 [\xi^2 e^{-v}]. \quad (15)$$

Taking corresponding values of ξ , $\xi(dv/d\xi)$, and $\xi^2 e^{-v}$ from Emden's tables we obtain a linear sequence of isothermal core solutions corresponding to a given mass M^*/M_\odot and temperature T^* . Plotting $\log \frac{1}{2}\rho^*_{\text{core}}$ against $\log r^*/R_\odot$ we obtain curves¹⁰ of the type shown by the heavy line in Fig. 2 which can be used for fitting with the corresponding curves for the inner face of the envelopes. These fitting curves are, of course, subject to homology transformations. For various core masses we have

$$r^* \sim M^*; \quad \rho^* \sim 1/M^{*2}. \quad (16)$$

A typical feature of these curves consists in the fact that they do not extend into the region of small radii but instead begin to spiral around a certain point in the $[\log \rho^*/2; \log r^*/R_\odot]$ plane. Physically this means that it is impossible to construct an isothermal core of an ideal gas with a radius smaller than a certain value determined by its mass. This fact underlies the above mentioned result of Chandrasekhar and his collaborators concerning the impossibility of building a stellar model with a core containing more than 10 percent of the mass. In fact, as we see from Fig. 2, the fitting curves for the envelopes (to be discussed in detail in the next section) cease to intersect the core curves when the mass of the envelope becomes smaller than 9 times the mass of the core.

B. The Case of a Partially Degenerate Gas

If, instead of considering the gas as ideal, we take into account the possibility of degeneracy, the equation of state³ has to be replaced by the equation of a partially degenerate gas. In this case we have

$$\rho = \frac{4\mu_e m_H (2\pi m_e K T)^{\frac{3}{2}}}{(\pi)^{\frac{1}{2}} h^3} F_{1/2}(\psi), \quad (17)$$

¹⁰ At the interface between the isothermal solution for the core and the radiative solution for the envelope we must have continuity of the gas pressure. Since the mean molecular weight of the core is assumed to be twice that of the envelope, the continuity condition requires that at this point $\frac{1}{2}\rho^*_{\text{core}} = \rho_{\text{env}}$.

$$P = \frac{KT(2\pi m_e KT)^{\frac{3}{2}}}{3(\pi)^{\frac{1}{2}} h^3} F_{3/2}(\psi) + \frac{a}{3} T^4, \quad (18)$$

where $F_{1/2}$ and $F_{3/2}$ are Fermi-Dirac functions defined by

$$F_\nu(\psi) = \int_0^\infty \frac{u^\nu du}{e^{-\psi+u} + 1}. \quad (19)$$

In the above expressions m_e and m_H are respectively the masses of an electron and of a proton, μ_e the effective molecular weight, and ψ a parameter determining the degree of degeneracy. The quantity k is the Boltzmann gas constant, and h is Planck's constant.

The equilibrium equations for an isothermal sphere described by the above equations of state have been integrated numerically by Wares¹¹ for different values of the parameter ψ_c . Using the Wares' solutions calculated for $\psi_c = 0, 2, 3, 5, 10, 20,$ and 100 , and transforming them to the conditions¹² $\mu_e = \mu_{\text{core}} = 2$ and $T = T^* = 2 \times 10^7 \text{K}$, we can again repeat the procedure of "cutting out" isothermal cores of a given mass M^* and plotting the logarithms of their surface densities $\frac{1}{2}\rho_{\text{core}}^*$ against the logarithms of their radii r^*/R_\odot . The resulting curve for $M^* = 0.1$ is shown by the heavy line in Fig. 2, and we see that in this particular case the spiraling part of the ideal gas curves does not have physical significance since degeneracy sets in before this solution for the polytrope is obtained. The fitting curve now continues into the region of smaller radii and gives well defined intersections with the envelope's curves corresponding to any percentage of star mass contained inside of the core. This removes the long standing paradox of the upper limit for the core mass. The complete set of core fitting curves which can be obtained from Wares' integrations is shown in Fig. 3 for core masses ranging from $0.0125 M_\odot$ to $0.40 M_\odot$. It shows that for small core masses the fitting curves continue monotonically from the ideal into the

¹¹ Gordon W. Wares, *Astrophys. J.* **100**, 158 (1944). We are grateful to Dr. Wares for kindly placing his unpublished and detailed tables representing the results of these integrations at our disposal.

¹² It may be noted here that Wares' solutions are calculated for a constant value of μ throughout the core. This is actually not quite correct since for the same chemical constitution the mean molecular weight in the degenerated part will be different from the value in the non-degenerated part. We have used Wares' data, however, since no better integrations are available at present.

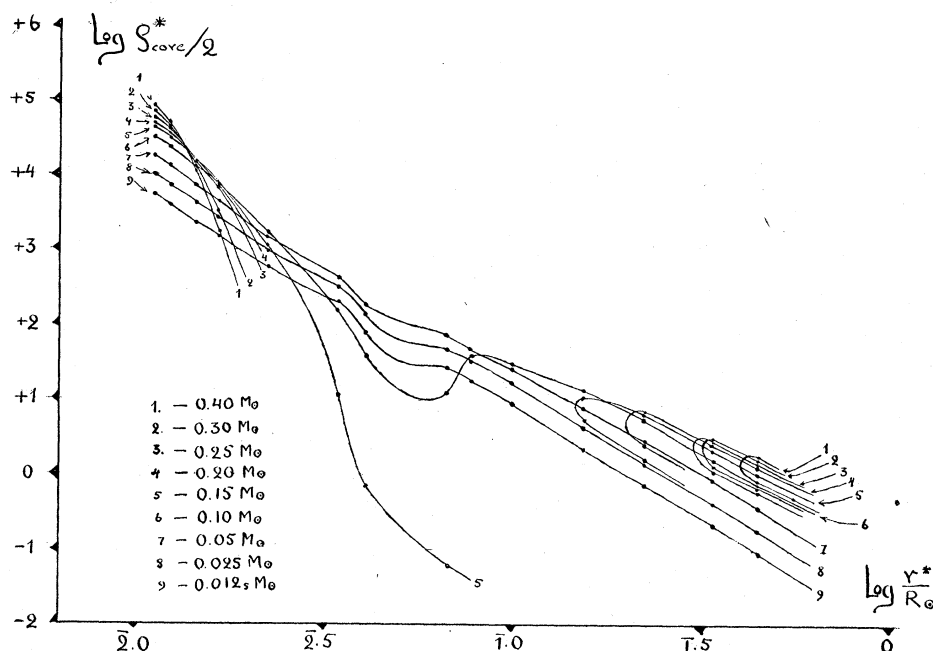


FIG. 3. Core fitting curves as obtained from Wares' data for various values of the core mass.

degenerate regions, whereas for larger masses (around $0.1 M_{\odot}$) we obtain a "folding" of the curve. For still larger masses the folding part goes a long way into the region of larger radii and its run in this region cannot be followed on the basis of the existing integrated solutions (mainly due to a large gap in Wares' tables between $\psi_c=20$ and $\psi_c=100$). However, as we shall see later, intersections with the fitting curves for the envelopes will also be present in this case. The lack of numerical solutions which can be used for cores with relatively large masses makes the study of the shell source evolution of massive stars more difficult than for smaller ones, and the further integrations of the equations of partially degenerated isothermal spheres become highly desirable.

3. SOLUTIONS FOR RADIATIVE ENVELOPES

For the radiative envelope of the star we have the equations

$$\frac{d}{dr} \left(-\frac{R}{\mu} \rho T + \frac{1}{3} a T^4 \right) = -\frac{GM(r)\rho}{r^2}, \quad (20)$$

and

$$\frac{d}{dr} \left(\frac{1}{3} a T^4 \right) = -\frac{KL\rho}{4\pi cr^2}, \quad (21)$$

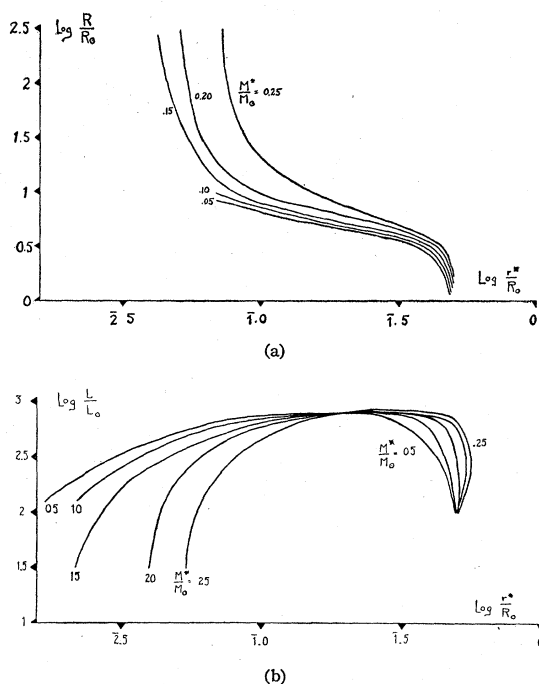
where the opacity coefficient K can be represented with a sufficient approximation by Kramers' formula

$$K = K_0 \rho T^{-3.5}. \quad (22)$$

Four numerical integrations of these equations have been performed by Strömgen.¹³ These integrations are carried out for a star with the mass, radius, and luminosity of the sun, a molecular weight $\mu = 2.2$ and the following values of the opacity coefficient K_0 : $\log K_0 = 26.2$; 27.0 ; 27.4 ; and 27.8 . The first two solutions "run out of mass" before reaching the center whereas the last two approach the center with an excess mass of 5 and 12 percent, respectively, of the total mass of the star. Transforming these solutions to a molecular weight $\mu = 1$, these solutions will hold exactly only if the mass is simultaneously transformed to $4.84 M_{\odot}$.¹⁴ Along with these four solutions we use a new solution calculated for $M = 4 M_{\odot}$, $R = 15 R_{\odot}$, $L = 10^4 L_{\odot}$, with the assumptions $\mu = 1$, $\log K_0 = 24.85$. This solution,

¹³ B. Strömgen, *Zeits. f. Astrophys.* **2**, 345 (1931).

¹⁴ Since the radiation pressure, which was taken into account in Strömgen's calculations, remains the same under the approximation $\mu^2 M = \text{constant}$.



FIGS. 4 (a) and (b). Relation of the radius and luminosity of a star of mass $4 M_{\odot}$ as a function of the radius and mass of the core. The curves are quantitatively rather approximate.

given in Table I, approaches the center with a mass excess of about 20 percent. It has been shown by Stromgren that the solutions which approach the center with a finite value of the mass can be extrapolated beyond the tabulated values to smaller radii by using the formulae

$$\rho \sim \left(\frac{1}{r}\right)^{32/11}; \quad T \sim \left(\frac{1}{r}\right)^{10/11};$$

$$M(r) \sim r^{-1/11} \quad (\text{for } r/R \ll 1). \quad (23)$$

These expressions show that $M(r)$ does not approach a finite value for $r=0$ but rather goes to zero very slowly. All the above solutions are free from convective instability, although in the case of the solution for $\log K_0 = 27.4$ one comes very close to such an instability.

Strictly speaking all the above solutions contain a term corresponding to the radiative pressure, and are not subject to homology transformations, being valid only for the values of M , R , L , ρ , and K_0 for which they are calculated. However, since a special integration of the equilibrium equations for each particular case re-

quires an enormous amount of work (about a hundred man hours per solution) we have used the homology transformations despite the approximation they involve.

If we choose for independent variables the mass M of the star, the temperature T at certain homological point, the molecular weight μ and the coefficient of opacity K_0 , the homology transformations for the remaining three variables become

$$r \sim \mu M / T, \quad (24)$$

$$\rho \sim T^3 / \mu^3 M^2, \quad (25)$$

$$L \sim \mu^7 M^5 T^{0.3} / K_0. \quad (26)$$

Using these formulae one must first transform Stromgren's solutions to the standard values of $\mu=1$ and $\log K_0 = 24.85$. In order to build an envelope for a given total mass of the star M , which can be fitted to a core with a mass M^* and temperature T^* , we must evidently choose from each of these tables a line corresponding to the prescribed value of M^*/M_{\odot} . Then, again using the above formulae, the solution is transformed so that the temperature corresponding to that value of M^*/M_{\odot} will become T^* , and the total mass of the star will become M . In this manner we get definite values from each solution for the inner radius r^* of the envelope, the density ρ^* at this point, and the corresponding radius R and the luminosity L of the envelope. These points determine a curve $[\log \rho^* \text{ vs. } \log r^*]$, the intersection of which with the $[\log (\rho^*/2) \text{ vs. } \log r^*]$ curve for the core will give us the fitting condition for the model.

It may be noticed here that whereas the core

TABLE I. Solution of the equations for the radiative envelope. $M=4M_{\odot}$; $R=15R_{\odot}$; $L=10,000L_{\odot}$.

$\log (r/R_{\odot})$	$\log \rho$	$\log (M(r)/M_{\odot})$	$\log T$
1.148	2.135-10	0.602	4.787
1.110	3.535	0.602	5.211
1.025	4.946	0.602	5.641
0.866	6.343	0.598	6.070
0.618	7.686	0.570	6.482
0.297	8.875	0.468	6.861
9.932-10	9.835-10	0.300	7.180
9.548	0.663	0.152	7.459
9.154	1.513	0.060	7.736
8.756	2.466	0.005	8.037
8.357	3.523	9.965-10	8.368
7.958	4.652	9.930	8.720
7.558-10	5.819	9.897-10	9.083

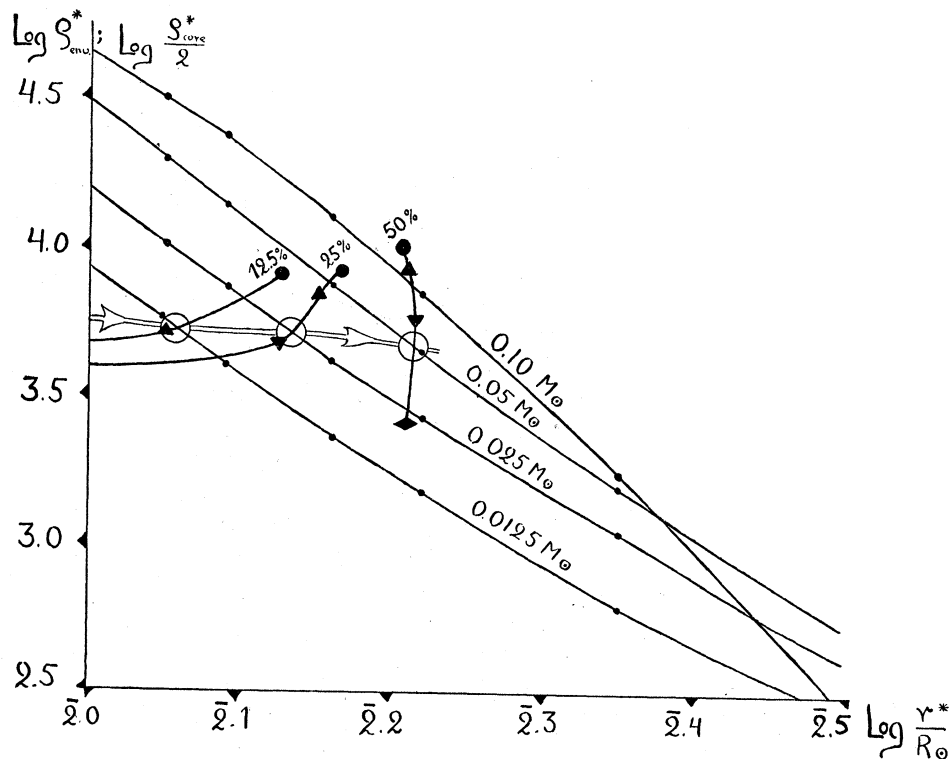


FIG. 5. Fitting curves for a star of mass equal to $0.1 M_{\odot}$. The notation is the same as that in Fig. 2. Intersections between corresponding curves are encircled.

curves are fixed, not being subject to homology transformations, the fitting curves for the envelopes can be constructed for one definite mass of the star M , and be moved for different star masses across the diagram in accordance with the conditions $r^* \sim M$, and $\rho^* \sim M^{-2}$.

The radius and luminosity of the star can now be determined directly from the value of the fitting radius. As an example we give in Figs. 4 (a) and (b) the dependence of R and L for a star of $4 M_{\odot}$ on the radius of the interface between the core and the envelope. For other star masses similar curves can be obtained by simple homology transformations.

4. SHELL SOURCE MODELS FOR STARS OF VARIOUS MASSES

As has already been mentioned, the peculiar character of the core fitting curves leads to qualitatively different results for the evolutionary tracks for stars of different masses. We will choose as our first example a star of very small

mass $0.1 M_{\odot}$, in which case the growth of the energy producing shell can be followed through the entire range from 0 to 100 percent of the total mass of the star. The corresponding part of the $[\log (\rho^*/2) \text{ vs. } \log (r^*/R_{\odot})]$ diagram is represented to an enlarged scale in Fig. 5 with the fitting curves for the cases in which the core contains 12.5, 25, and 50 percent of the mass of the star. The radii and luminosities obtained from the three intersections are shown in the frame of the ordinary $[\log (L/L_{\odot}) \text{ vs. } \log (R/R_{\odot})]$ diagram in Fig. 8. In this diagram the general direction of the main sequence and the locations of some well-known stars are also indicated for the sake of comparison. We see that in this case the shell source model does not experience any considerable increase of stellar radius in any stage of its evolution. The representative point of the star evolves through regions slightly off the main sequence in the direction of increasing radii and luminosity, following for a while the continuation of the track calculated by Schön-

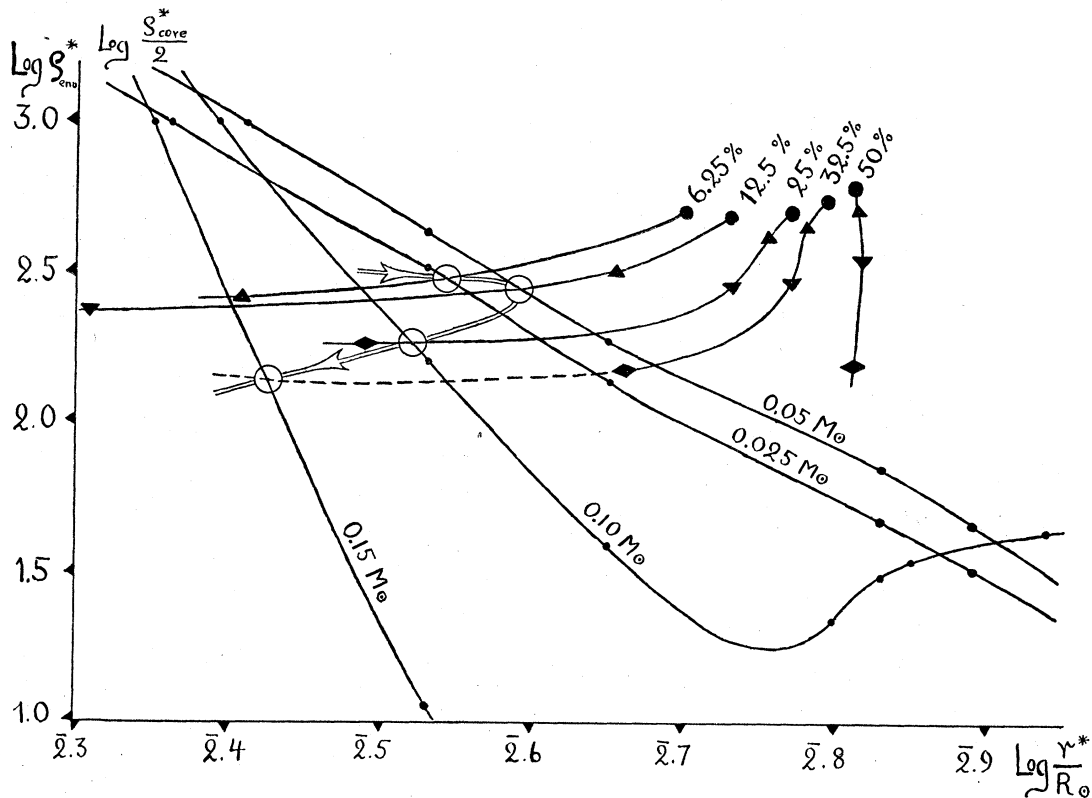


FIG. 6. Fitting curves for a star of mass equal to $0.4 M_{\odot}$. The notation is the same as in Fig. 2. Intersections between corresponding curves are encircled.

berg and Chandrasekhar. With further increase of the mass of the core the radius of the star begins to decrease while its luminosity continues to increase, and (when the mass of the core is about 50 percent) the star crosses the main sequence line. With the gradual approach of the energy producing shell to the surface of the star, its effective temperature rises very rapidly, and one may expect the ejection of the outer layers to begin at a certain point during the subsequent evolution. A more detailed study of these late stages of shell source evolution will represent the subject of a later publication.

As a second example we will consider a star with a total mass $0.4 M_{\odot}$. In this case the existing integrated solutions permit a study of the evolution only up to the point where the core contains about 32 percent of the star's mass. From Fig. 6, representing the fitting curves for that particular case, we see that whereas the intersections corresponding to 6.25 and 12.5

percent of the mass are similar to those in the previous case, the situation changes quite essentially when the shell continues to grow. In fact, due to beginning of "looping" in the core curves, the intersection points begin to move towards smaller core radii, which results in a rapid increase in the stellar radius and luminosity. The evolutionary track for a star of that mass is shown in Fig. 8, and we notice that for a core containing 32.5 percent of the mass the radius of the star has increased by a factor of about 40, its luminosity becoming more than tenfold its original value. Further stages in the evolution cannot be followed at present because of the lack of suitable integrated solutions.

Both examples discussed above are of purely theoretical interest and cannot be compared with actual stars, since stars of such small mass consume their original hydrogen content very slowly, and can hardly be expected to have reached the advanced stage of evolution predicted here at

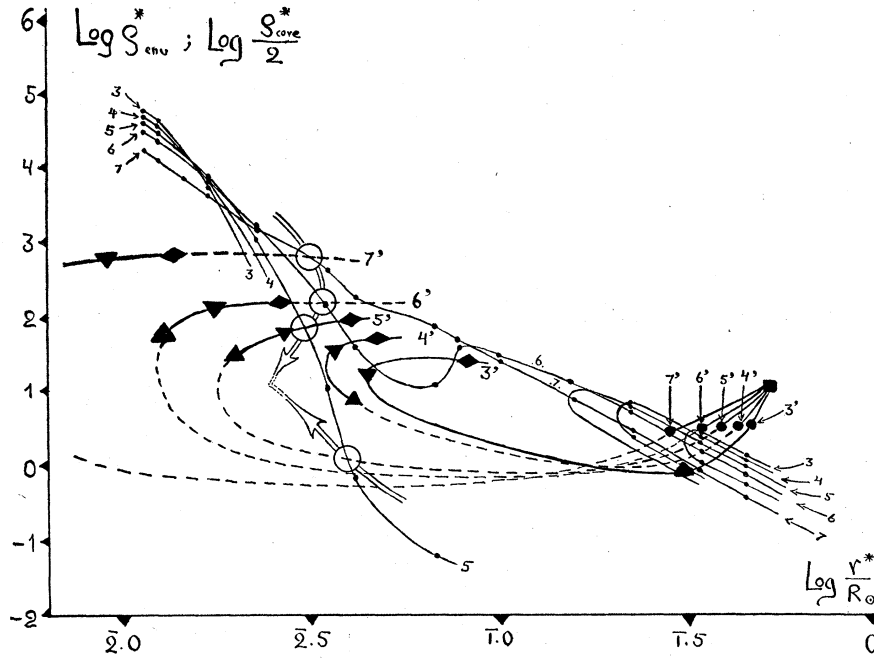


FIG. 7. Fitting curves for a star of mass equal to $4 M_{\odot}$. The notation is the same as in Fig. 2 and Fig. 3 with an additional point from one of Strömberg's "negative mass" solutions indicated by the square. (The "square" points corresponding to different envelopes are so close together that they cannot be distinguished on the diagram.)

the present age (a few billion years) of the stellar universe. They indicate however that the growth of an energy producing shell can cause a considerable increase in stellar radius, an increase which becomes more pronounced for the stars of larger mass.

The most interesting case corresponds, of course, to stars several times heavier than the sun, since the stars in this mass range have used by now a large proportion of their original hydrogen supply and must be expected to be found at present in an advanced stage of their evolution.

The fitting curves corresponding to a star of mass $4 M_{\odot}$ are shown in Fig. 7. For convenience we shall discuss the evolutionary stages corresponding to various core masses separately.

A. Core Mass $M^* = 0.05 M_{\odot}$

It is to be noted that the fitting curve for the core (No. 7) is a monotonically decreasing function, and that consequently along all points of this curve an infinitesimal decrease in the radius implies an increase in the surface pressure. It is

reasonable to suppose that this means that the core will be stable to small fluctuations of the pressure on the surface. There is an intersection at the lower right side of the graph corresponding to a star of $\log L = 2.9 L_{\odot}$ and $\log R = 0.65 R_{\odot}$. It will be found that such a star lies well within the main sequence. This star has a core of isothermal gas in a nearly perfect gas condition, and is one which has already been described by Schönberg and Chandrasekhar.⁵

B. Core Mass $M^* = 0.10 M_{\odot}$

Observing first the structure of the curve for the isothermal core (No. 6), one notices the existence of a region near $\log (r^*/R_{\odot}) = 0.875$ where the value of $d\rho^*/dr^*$ is positive. This implies that if the core were in a condition represented by a point in this region of the curve, the core would begin to collapse spontaneously if the pressure on its surface did not decrease too rapidly as the core contracted. For the star under consideration, however, the envelope curve intersects the core curve in only two points, at both of which the slope of the core

curve is negative. The intersection on the lower right is similar to the adjacent point for a core mass of $0.05 M_{\odot}$, and represents a later stage in the evolution of a star of this type. The radius and luminosity of the star have not changed appreciably, and consequently the star remains at about the same point on the main sequence and on the Hertzsprung-Russell diagram of Fig. 8. There is an additional intersection at the upper left-hand side of Fig. 7 which deserves some attention. It will be seen that the radius of the core is very small in this case and that its surface density is exceedingly high. The material in the core is highly degenerate. Unfortunately the existing integrations of the radiative envelope equations do not allow very accurate estimates of the radius and luminosity of the corresponding star to be made, but these appear to be about $\log(L/L_{\odot}) = 2.5$ and $\log(R/R_{\odot}) = 1.5$. It will be seen that this star is truly a red giant.

C. Core Mass $M^* = 0.15 M_{\odot}$

In this case the curve for the isothermal core has a break in the middle, the right-hand branch turning back on itself approximately as shown. As one traces the upper right-hand branch toward the left, around and back to the right along the lower right-hand branch, one proceeds in the direction of increasing degeneracy of the core. We do not have enough information to say just how the curve behaves beyond the right-hand margin, but one can pick the curve up again at the lower end of the left-hand branch and proceed, still in the direction of increasing degeneracy, upward and to the left. It appears that the values of the density corresponding to points in the break between the two curves are quite small. The peculiar behavior of the curve is caused by the fact that in the region where the right-hand branch turns back on itself the gravitational attraction of the matter in the star for itself has become so great that the rate of increase of the internal gas pressure with decreasing radius of the star becomes smaller than the gravitational force of contraction, and the core tends to collapse. This brings about a redistribution of matter in the core with an increasing concentration of matter in the center and a reduced density on the surface. Apparently

the reduction of density near the surface of the core is more effective in reducing the mean density of the core than the increased density near the center is in increasing it, since as one proceeds along the lower right-hand branch the core must have increasingly larger radii in order to contain the required mass of $0.15 M_{\odot}$. Jumping to the left-hand branch one comes to cores which are so highly degenerate that they have become relatively less compressed again, and the surface density and pressure must increase rapidly as the radius of the core is reduced.

It will be seen that the envelope curve intersects the core curve in four places. The upper right-hand intersection is analogous to the right-hand intersections in the case of lighter cores. The lower right-hand intersection implies the possible existence of another star, the radius and luminosity of which do not differ greatly from those corresponding to the upper right intersections. There are two intersections with the left-hand branch, both corresponding to relatively small luminosities and to very large radii. The values of the latter quantities have been estimated very roughly from Fig. 4, enabling points representing these two star models to be plotted in Fig. 8. The upper left-hand intersection is, of course, of the same kind as the left-hand intersections corresponding to the smaller core masses, whereas the lower left-hand intersection represents a new possible stellar model.

D. Core Masses $M^* = 0.20 M_{\odot}$ and $0.25 M_{\odot}$

The core curves for these two masses are similar to that for a core of mass $M^* = 0.15 M_{\odot}$, except that because of the larger masses the collapse of the core (corresponding to the turning back point of the right-hand branch) occurs at a larger radius. Similar considerations explain the behavior of the left-hand branches. In these two cases no left-hand intersections exist, but the right-hand ones are present as before.

E. Cores with Masses Greater than $0.40 M_{\odot}$

It will be seen from Fig. 7 that in this case no intersections exist between the envelope fitting curves and either branch of the core fitting curve. Apparently there are no solutions in this

case. The situation is not unlike that described by Chandrasekhar and Schönberg for their model with a core of a perfect gas. Even assuming the possibility of a core of degenerated gas it apparently is not possible to obtain a fit for stars of this mass.

It is desirable at this point to attempt to link the possible solutions for various different core masses together in an evolutionary sequence. This has been done in a rather mathematical fashion in Fig. 7 for the left-hand solutions simply by drawing curves through adjacent points of intersection, thus producing two possible evolutionary tracks. The same might be done for the two right-hand solutions, but to do so would clutter up the diagram. The question now arises as to which track is the correct one, whether transitions from one track to another can occur, and what happens when the mass of the core exceeds that for which suitable solutions exist. Aside from a certain reasonableness, the following suggested evolution is largely conjecture on the part of the authors.

It is probable that the star begins its evolution with a relatively rarefied core corresponding to the upper right-hand intersections (Chandrasekhar-Schönberg solutions). This stage of evolution may be modified by a certain amount of energy production throughout the core as a result of the convective mixing of the unconsumed hydrogen with the rest of the core material.

As soon as the star reaches the stage of evolution where the core is represented by a point on a core curve for which $d\rho^*/dr^*=0$ there will be a tendency for the core to contract through a series of non-isothermal equilibrium states, at a rate corresponding to the Kelvin Helmholtz time scale. Since such a contraction of the core should be a slow process, then, corresponding to the slow decrease in the radius of the core there would necessarily be a slow increase in the radius of the star as will be seen from Fig. 4a. This result is easily obtained if one assumes that the envelope is in radiative equilibrium and calculates what will happen to the radius as the core radius is decreased, assuming constant surface temperature and mass for the core. The expanding star will gradually become a red giant and possibly a supergiant. Whether the star ever reaches a condition corresponding to the

left-hand intersections is problematical. It does not appear to happen in the case of stars of mass $M=4 M_{\odot}$, since the left-hand intersections cease to exist before the upper right-hand intersections reach the unstable portion of a core curve.

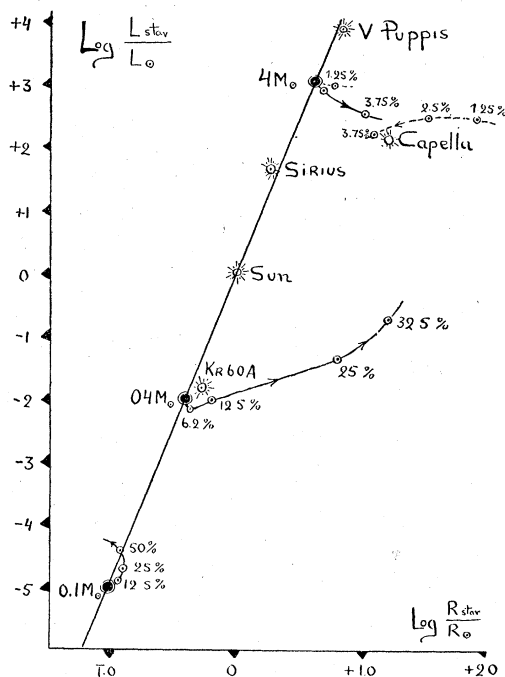


FIG. 8. Evolutionary tracks calculated for the stars of 0.1, 0.4, and $4 M_{\odot}$. The values of the radii of the stars on the $4 M_{\odot}$ curve are very uncertain and could be actually much larger than indicated.

CONCLUSIONS

The results obtained in the previous section indicate that the growth of the energy producing shell within a sufficiently massive star may lead to a very large increase of stellar radius, thus bringing the star into the region of the Hertzsprung-Russell diagram occupied by the red giant and supergiant stars. It is tempting, therefore, to consider the stars of these groups as representing various stages of hydrogen shell source evolution, particularly in view of the fact that there is, as it seems, no other adequate explanation of their existence. In fact, it is not possible to consider stars of the red giant branch as still being in the stage of gravitational contraction since in this case their radii would be

decreasing at a faster rate than is consistent with the observational evidence.¹⁵ On the other hand, the attempt by Gamow and Teller¹⁶ to explain the energy production in red giants as caused by thermonuclear reactions involving light elements (Li, Be, B) cannot explain the peculiar distribution of these stars in the Hertzsprung-Russell diagram; in fact, one would expect in this case that the stars would be distributed in different bands running parallel rather than almost perpendicular to the main sequence. Thus, although it is very possible that some of the red stars scattered through this region of the Hertzsprung-Russell diagram are still consuming their original allotment of light elements, the main bulk of the stars forming the so-called red branch require a different explanation. A look at the general position of the red branch, especially in the case of Baade's stellar population of type II¹⁷ suggests on the other hand that most red stars represent evolutionary stages subsequent to the main sequence; in fact, only in such a case would the brighter, faster evolving, stars get farther away from their main sequence position. The above discussed features of shell source evolution seem to fit rather well with the general picture as it presents itself on the basis of observational data. It may be noticed that the appearance of a red giant branch for more massive stars does not even require the assumption that they have consumed a larger portion of their hydrogen, since, as we have seen in the previous section, only such massive stars are at all able to expand considerably beyond their normal size in the main sequence. Thus it may turn out that the absence of highly expanded stars of comparatively small mass is not at all connected with the slowness of their evolution, but is rather due to the peculiar properties of partially degenerated shell source models for small masses. On the other hand it seems very likely that the difference between the red giant branches in the two types of stellar population is directly connected with the age of these particular stellar groups. It would seem that the absence of diffuse interstellar material in the

regions occupied by stellar population of the type II indicates that the stars of that group are, on the average, older than the stars of type I. It must be hoped that a further, more detailed study of the shell source model for heavy stars will explain the striking differences between these two types of stellar population. It may be noted in conclusion that the calculations presented in the present article must be considered as of only provisional nature, in particular because of the rigid assumptions made about the temperature in the energy producing shell, and concerning the values of the molecular weights in the core and in the envelope. The solutions of partially degenerate cores are invariant in respect to changes of mass, temperature, and molecular weight for which the product $M^* \mu_{\text{core}}^* (T^*)^{-2} = \text{a constant}$, so that assuming different values of T^* and μ_{core} we obtain similar solutions for different core masses M^* . In particular, assuming, as it seems very likely at present,¹⁸ that stellar material consisted originally almost entirely of hydrogen and helium (55 percent H; 40 percent He; less than 5 percent Russell mixture) we would have to use $\mu = 0.7$ for the envelope and $\mu = 1.4$ for the core. Using $\mu = 1.4$ instead of $\mu = 2$ for the core we will find that the "looping phenomenon" of the $[\log(\rho^*/2) \text{ vs. } \log(r^*/R_{\odot})]$ curves (compare Section 2) will take place only for core masses $(2/1.4)^2 \approx 2$ times as large, so that the evolutionary track for a star of about one sun mass will now look similar to that calculated by us for $0.4 M_{\odot}$. Other important changes in the values of star masses corresponding to an evolutionary track of a given shape will result from the change of the value of T^* , which, of course, need not necessarily be exactly the same in the energy producing shell as it is in the center of a point source model. The work of improving present calculations in the above indicated directions, with the aim of getting a closer comparison with the observational data is now in progress.

Previously reported difficulties connected with the construction of shell source stellar models containing a large fraction of the total mass in the isothermal core arise in part from the arbi-

¹⁵ G. Gamow, Phys. Rev. **55**, 718 (1939).

¹⁶ G. Gamow and E. Teller, Phys. Rev. **55**, 791 (1939); Compare also M. Greenfield, Phys. Rev. **60**, 175 (1941).

¹⁷ W. Baade, Astrophys. J. **100**, 137 (1944).

¹⁸ Compare G. Gamow and J. A. Hynek, "The review of Weizäcker's planetary theory," Astrophys. J. **101**, 249 (1945).

trary assumption that the material of the core should be treated as an ideal non-degenerate gas. The picture changes materially when one takes into account the possibility of the existence of degeneracy near the center of the core. Models obtained by fitting a partially degenerated isothermal core to the radiative envelope are not subject to homology transformations in respect to the mass, and their evolutionary behavior presents essentially different features for small and large star masses. In the case of very small star masses ($\sim 0.1 M_{\odot}$), the observable characteristics of the shell source star show only comparatively small deviations from the values corresponding to the main sequence position. With the fraction of the total mass in the core increasing up to 50 percent, the luminosity of the model increases by a factor of 4, whereas its radius shows first a slight increase (by about 13 percent) and then begins to decrease. Beyond this stage the evolution is represented most probably by a continuous decrease of both radius and luminosity towards values corresponding to completely degenerated white dwarf configurations. For larger star masses ($\sim 0.4 M_{\odot}$) the picture of evolution looks quite different, and the growth of the core results in a very large increase of the stellar radius. It has been calculated that for a star with 32 percent of the total mass in the core, the radius becomes 40 times as large and the luminosity 20 times as large as they

would be were the star in the main sequence. For still larger masses ($\sim 4 M_{\odot}$) the situation is considerably more complicated because of the fact that in this case a given core mass corresponds to several possible configurations, which can presumably evolve from one to another through a process of internal rearrangement of the stellar material and the liberation of gravitational energy. Although it has not been possible in this case to follow the entire evolutionary track owing to the lack of a sufficient number of integrated solutions, the available results indicate that when a relatively small core mass has been reached the radius of the star will begin to increase to a very large value and the luminosity will simultaneously decrease. It is suggested that stellar models with steadily growing cores and shell sources of energy can be used for the explanation of internal structural features and the evolutionary development of the group of giant and supergiant stars.

ACKNOWLEDGMENTS

The authors consider it a pleasure to express their thanks to Dr. H. Polaček and Mrs. Cynthia Watkins for performing the numerical integration (given in Table 1) of the radiative equilibrium equations and to Mrs. E. Keller for assistance with various calculations and general preparation of the manuscript.